Received: 18 July 2022 | Revised: 14 March 2023 | Accepted: 17 March 2023

DOI: 10.1002/eco.2545

RESEARCH ARTICLE

WILEY

Importance of tree diameter and species for explaining the temporal and spatial variations of xylem water $\delta^{18}O$ and $\delta^{2}H$ in a multi-species forest

Maëlle Fresne[1,2] | Kwok P. Chun[3] | Markus Hrachowitz[4] | Kevin J. McGuire[5] | Remy Schoppach[1,6] | Julian Klaus[7]

[1]Catchment and Eco-Hydrology Research Group, Environmental Research and Innovation Department, Luxembourg Institute of Science and Technology, Belvaux, Luxembourg

[2]Agri-Food and Biosciences Institute, Belfast, UK

[3]Department of Geography and Environmental Management, University of the West of England, Bristol, UK

[4]Department of Water Management, Faculty of Civil Engineering and Geosciences, Delft University of Technology, Delft, The Netherlands

[5]Department of Forest Resources and Environmental Conservation and Virginia Water Resources Research Center, Virginia Tech, Blacksburg, Virginia, USA

[6]Université Catholique de Louvain, Louvain-la-Neuve, Belgium

[7]Department of Geography, University of Bonn, Bonn, Germany

Correspondence
Maëlle Fresne, Agri-Environment Branch, Agri-Food and Biosciences Institute, Belfast, UK.
Email: maelle.fresne@hotmail.fr

Funding information
Luxembourg National Research Fund, Grant/Award Number: FNR/CORE/C17/SR/11702136/EFFECT; Accelerator Programme (AP) 2022-24; University of the West of England, Bristol

Abstract

Identifying the vegetation and topographic variables influencing the isotopic variability of xylem water of forest vegetation remains crucial to interpret and predict ecohydrological processes in landscapes. In this study, we used temporally and spatially distributed xylem stable water isotopes measurements from two growing seasons to examine the temporal and spatial variations of xylem stable water isotopes and their relationships with vegetation and topographic variables in a Luxembourgish temperate mixed forest. Species-specific temporal variations of xylem stable water isotopes were observed during both growing seasons with a higher variability for beeches than oaks. Principal component regressions revealed that tree diameter at breast height explains up to 55% of the spatial variability of xylem stable water isotopes, while tree species explains up to 24% of the variability. Topographic variables had a marginal role in explaining the spatial variability of xylem stable water isotopes (up to 6% for elevation). During the drier growing season (2020), we detected a higher influence of vegetation variables on xylem stable water isotopes and a lower temporal variability of the xylem water isotopic signatures than during the wetter growing season (2019). Our results reveal the dominant influence of vegetation on xylem stable water isotopes across a forested area and suggest that their spatial patterns arise mainly from size- and species-specific as well as water availability-dependent water use strategies rather than from topographic heterogeneity. The identification of the key role of vegetation on xylem stable water isotopes has critical implications for the representativity of isotopes-based ecohydrological and catchments studies.

KEYWORDS
principal components, spatial autocorrelation, stable water isotopes, topography, transpiration, vegetation

Significance statement

Understanding water sources and water use by trees is critical for forest management and sustainability especially in the context of global change. To date, there is no clear relationships

between patterns of tree water uptake (informed by the isotopic composition of tree stems) and variations of vegetation and topography in the landscape. Therefore, we sampled tree trunk water of around 350 trees scattered across a forested area in Luxembourg to study how water uptake differed between trees and how it was related to the vegetation (tree species and diameter) and the topography (e.g. elevation and slope).

1 | INTRODUCTION

Vegetation critically affects soil water fluxes and the terrestrial water balance (Brutsaert, 1988) through interception and root water uptake for transpiration (Moore & Heilman, 2011; Rodriguez-Iturbe, 2000). Global change poses a considerable challenge for forest and water resource management due to shifts in precipitation regimes and temperatures that may affect tree water uptake and plant water availability (e.g. Capell et al., 2013), species composition and distribution (Tetzlaff et al., 2013) and forest productivity (Boisvenue & Running, 2006). Therefore, an improved understanding of the influence of biotic and abiotic factors on tree water uptake is needed to better evaluate the variations of tree water use (Frank et al., 2015) and manage forest ecosystems to enhance their adaptive response to environmental stressors.

Stable isotopes of oxygen (ratio of ^{18}O to ^{16}O) and hydrogen (ratio of ^{2}H to ^{1}H) of water have been widely used to understand hydrological and ecohydrological processes in catchments (e.g. Bögelein et al., 2017; Brinkmann et al., 2018; Fabiani et al., 2021; Goldsmith et al., 2012, 2018; Penna et al., 2018; Sprenger et al., 2016, 2018; Tetzlaff et al., 2020). They are an important tool for describing the movement of water through catchments and ecosystems (Kendall & McDonnell, 1998; Klaus & McDonnell, 2013). Stable water isotopes (SWI) have proved to be essential for investigating water fluxes in the soil–plant–atmosphere continuum (e.g. Fabiani et al., 2021; Goldsmith et al., 2012), flow paths and associated transit times of water in the subsurface (Asadollahi et al., 2022; Knighton et al., 2019; Sprenger et al., 2016), along hillslopes (Asano & Uchida, 2012) and in catchments (Kuppel et al., 2018; Rodriguez & Klaus, 2019; Sprenger et al., 2022; Wang et al., 2023) showing their potential to decipher water movements in the critical zone. Analysing SWI in plant stem water (usually assumed to be xylem water) is important for quantifying water sources and water use by plants (Penna et al., 2018).

Xylem water is a mixture of the different water sources used by trees (i.e. soil water from different depths and groundwater) (Penna et al., 2018). The variations of xylem SWI are therefore related to variations in these sources and how they are taken up by trees. The temporal variability of xylem SWI is related to soil SWI that are themselves modified *via* mixing with infiltrating rainwater with its own interstorm and intrastorm variation in isotopic composition (Bertrand et al., 2014; Sprenger et al., 2018). Additional temporal drivers of xylem SWI are meteorological conditions (e.g. air temperature, net radiation and humidity) that influence evaporation–fractionation of soil SWI (e.g. Bertrand et al., 2014). Vegetation characteristics such as species, forest type, tree height, diameter and above ground biomass (e.g. Fabiani et al., 2021; Goldsmith et al., 2012, 2018; Snelgrove et al., 2021) also influence xylem SWI. The effect of vegetation variables on xylem SWI is attributed to possible species-specific differences in the timing and intensity of water use (Snelgrove et al., 2021) or depth of water uptake (e.g. Brinkmann et al., 2019; Fabiani et al., 2021; Goldsmith et al., 2022; Kahmen et al., 2021).

Some studies addressed the spatial variability of xylem SWI at plot (Goldsmith et al., 2018), hillslope (Fabiani et al., 2021; Goldsmith et al., 2012) and catchment (Gaines et al., 2016) scales relying on 12 to 60 trees sampled on the same day. Those studies showed that xylem SWI were influenced by soil depth at the tree location, vegetation variables (e.g. Gaines et al., 2016) and the depth and lateral distributions of soil SWI (Gaines et al., 2016; Goldsmith et al., 2018). Spatial variations of soil SWI can themselves be related to topography (e.g. aspect, slope and elevation) that affect water movement in soil, energy inputs for evaporation and in consequence soil SWI. Topography (e.g. elevation) can also influence patterns in vegetation, the depth and accessibility of tree water sources and, in turn, tree water uptake depth and xylem SWI. Beyer and Penna (2021) emphasised that spatial data of xylem and soil SWI are scarce. For this reason, we are lacking an understanding of the relationship between xylem SWI and topographic and vegetation variables. Particularly, it remains unclear what is the relative importance of topographic and vegetation variables in explaining the spatial variability of xylem SWI.

In this study, we address this need by exploring the temporal and spatial variations of xylem SWI and their relationship with vegetation and topographic variables in a mixed beech-oak forest. We measured $\delta^{18}O$ and $\delta^{2}H$ of xylem water over two growing seasons (17 sampling campaigns) in ~350 trees in the Weierbach catchment, Luxembourg. We went beyond the sampling strategy generally used in ecohydrological studies (i.e. four tree individuals per species on average on each sampling campaign; Goldsmith et al., 2018) and sampled on average, for each sampling campaign, 10 tree individuals per species. To the best of our knowledge, this was the first analysis with more than 300 xylem samples determining the relative importance of vegetation and topographic variables in explaining the spatial variability of xylem SWI and highlighting its interannual change. The high total number of xylem samples taken within the 42-ha forested area provided a high sampling density (>3.3 trees/ha per growing season) and variations in vegetation and topography on which we based the spatial analysis.

Our research questions are guided by a perceptual model of the influence of vegetation and topography on xylem SWI. We know that species influence xylem SWI through its effect on tree water uptake depth (e.g. Fabiani et al., 2021). We also know that tree diameter at breast height (DBH) is associated with depth of tree water uptake (e.g. Schoppach et al., 2021), and we thus expect DBH to influence

xylem SWI. Specifically, in the Weierbach catchment, trees rely on soil water with no significant uptake of groundwater (Fabiani et al., 2021). Soil water availability is linked to vertical and lateral redistribution mechanisms of infiltrating water along the hillslope (Hissler et al., 2021; Rodriguez & Klaus, 2019), and we therefore believe that elevation, TPI and slope influence tree water uptake depth and, in turn, xylem SWI. We also expect these variables, along with aspect, to influence xylem SWI by affecting evaporation–fractionation of soil SWI. Multiple landscape variables can therefore affect xylem SWI, and their possible interactions are challenging to untangle their respective influence on xylem SWI. We hypothesize that xylem SWI vary systematically following the perceptual model; we address this hypothesis by investigating the following research questions:

1. How does the variability of xylem SWI over a growing season change between species?
2. How do species influence the systematic spatial variation of xylem SWI?
3. What is the relative importance of vegetation and topographic variables in explaining the spatial variability of xylem SWI?
4. How do the relationships between xylem SWI and tree size, species, and topographic variables differ between growing seasons?

2 | MATERIALS AND METHODS

2.1 | Study area

The Weierbach is a 42-ha forested headwater catchment located in the northwest of Luxembourg (Hissler et al., 2021) (Figure 1). The region is characterised by gently sloping plateaus cut by deep V-shaped valleys. Two landscape units are distinguished depending on their subsolum type and their slope: plateaus (about 30 ha, slopes between 0° and 5°) and hillslopes (about 12 ha, slopes between 5° and 44°) (Martínez-Carreras et al., 2016). Furthermore, there is a small riparian zone of up to 3-m wide surrounding most of the stream network and representing about 0.4 ha (Glaser et al., 2020).

Detailed topographic variables were calculated from a high-resolution (1 m) digital elevation model (DEM) (Luxembourgish air navigation administration, 2017) and included aspect (°), slope (°), curvature (–) and drainage area (m^2) for each 1 × 1 m DEM pixel. The aspect represents the direction the downhill slope faces (measured clockwise from 0 (north) to 360° (north)), the slope represents the steepness, the curvature indicates if the surface is upwardly convex (positive value), concave (negative value) or flat (value of 0) and the drainage area indicates the area from where water flows downslope (Schoppach et al., 2021) (Table 1). Based on these variables, the topographic position index (TPI; –) and topographic wetness index (TWI; ln(m)) were calculated (Wilson & Gallant, 2000) as follows:

$$\mathrm{TPI} = E - E_{avg50}$$

where E is the elevation at a specific location (m) and E_{avg50} is the average elevation in a 50 m radius circle around this location (m). The TPI value decreases from the catchment ridges to valley.

The TWI characterises terrain-driven propensity for saturation and is calculated as follows:

$$\mathrm{TWI} = ln\left(\frac{A_s}{\tan\beta}\right)$$

where A_s is the specific area (i.e. drainage area per unit contour length) in $m^2\ m^{-1}$ and β is the slope in °.

The bedrock in the Weierbach catchment consists mostly of Devonian slate containing schist, phyllite, and quartzite (Juilleret et al., 2011). Pleistocene periglacial slope deposits cover the bedrock, and the soil developed from these deposits is Leptic Cambisol (Juilleret et al., 2011) according to the World Reference Base classification. The weathered and fractured bedrock starts on average at about 140-cm depth, with fractures closing at approximately 5-m depth (Gourdol et al., 2021).

The semi-oceanic climate at the Weierbach catchment is governed by the interplay between seasonality in precipitation and evapotranspiration (ET; Pfister et al., 2017). Precipitation averaged 783 mm/year (2006–2018) and is rather uniformly distributed throughout the year. The average annual stream discharge is 478 mm (2006–2014; Pfister et al., 2017) with lower base flow occurring from July to September due to higher losses through ET (potential ET annual average of 593 mm for the period 2006–2014; Pfister et al., 2017). Snow can accumulate for a few days in winter, but it generally melts within a few days.

The vegetation in the Weierbach catchment is dominated by uneven-age deciduous hardwood trees (70% of the catchment area; European Beech *Fagus sylvatica* and Oak *Quercus petraea x robur*) and pure plantations of conifers (30% of the catchment area; European Spruce *Picea abies* and Douglas fir *Pseudotsuga menziesii*) (Fabiani et al., 2021; Hissler et al., 2021) located in some areas of the catchment (Figure 1). The deciduous hardwood trees rely on soil water with no significant groundwater uptake (Fabiani et al., 2021). Tree DBH of selected trees was measured within a 360 m × 20 m inventory plot located in the beech-oak stand (Table 1; Schoppach et al., 2021).

2.2 | Hydrometeorological monitoring and isotopic measurements

Precipitation volumes (P) and air temperature (T) over the study period were measured every 15 min at the Roodt station (Figure 1) following the World Meteorological Organization standards (Sevruk et al., 2009); we computed the daily total P and daily average T. Gaps in the daily P time series (6% over 2019–2020) were filled using a linear regression between daily P at the Roodt and Holtz (located about 2.6 km from the Roodt station; operated by the Water Agency of Luxembourg) stations (2015–2020; $R^2 = 0.47$, $p < 0.05$). Total annual P was equal to 1030 mm in 2019 (506 mm over the growing season—1 April to 31 October) and 957 mm in 2020 (404 mm over the

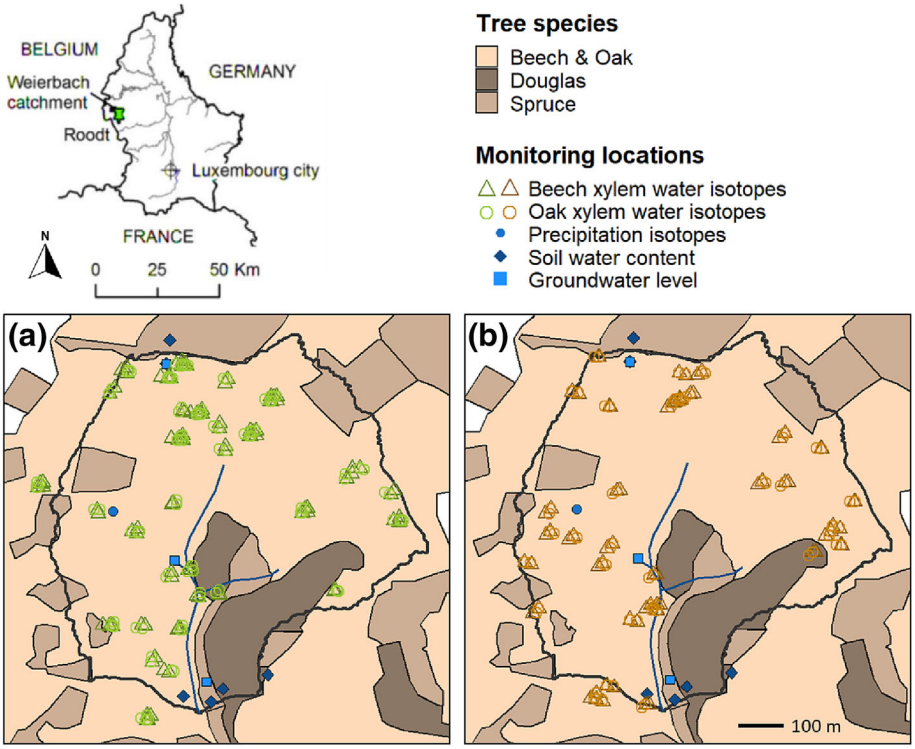

FIGURE 1 Locations of sampled beech and oak trees within the Weierbach catchment during the studied years 2019 (a) and 2020 (b). The map on the upper left shows the location of the Weierbach catchment in Luxembourg and of the Roodt station (green symbol).

TABLE 1 Distribution of topographic variables and vegetation characteristics in the studied catchment and at the tree sampling locations.

		Range at the tree sampling locations	
	Range in the studied catchment	2019	2020
Topographic variables			
Elevation (masl)	460–512	473–513	471–513
Aspect (°)	45–337	58–241	65–284
Slope (°)	0.6–31	2–27	1–27
Curvature (–)	−9.8 to 8.1	−2.2 to 1.2	−0.8 to 1.5
Drainage area (m^2)	3–29,735	6–12,700	10–12,329
TPI (–)	−6.8 to 4.6	−0.5 to 0.3	−0.8 to 0.5
TWI (ln(m))	2.4–14.1	0.1–6.9	0.3–7.0
Vegetation characteristics			
DBH (cm)	Beech: 3–75[a]	Beech: 3–89	Beech: 24–71
	Oak: 24–66[a]	Oak: 29–91	Oak: 30–79

[a]Measured within a 360 m × 20 m inventory plot.

growing season) (Figure 2a). The annual average T was 9.6°C in 2019 (13.8°C over the growing season) and 10.9°C in 2020 (14.4°C over the growing season) (Figure 2b).

Volumetric soil water content (SWC) was measured every 30 min at six locations across the catchment (Figure 1) with CS650 reflectometers (Campbell Scientific Ltd, Logan, UT, USA). At each location, eight probes were installed parallel to the surface at 10, 20, 40, and 60 cm depth (two probes per depth) (Hissler et al., 2021). For each location, we calculated the mean SWC value across all depths and then the daily mean SWC. Depth to groundwater level (DGWL) was measured every 15 min at three locations across the catchment (Figure 1) with OTT Orphimedes and CTD (Hissler et al., 2021); we calculated the daily mean DGWL for each location. For SWC and DGWL, we determined the catchment daily average as the mean value of all locations. The annual average SWC was 0.156 $m^3\ m^{-3}$ in 2019 (0.129 $m^3\ m^{-3}$ over the growing season) and 0.148 $m^3\ m^{-3}$ in 2020 (0.114 $m^3\ m^{-3}$ over the growing season) (Figure 2c). The annual average DGWL was 1.6 m in 2019 and 1.7 m in 2020 (1.8 and 1.9 m over the growing seasons, respectively) (Figure 2d).

Precipitation was sampled fortnightly for SWI analysis at one location in the catchment (Figure 1) using a 3-L Palmex rain sampler, which minimises gas transfer between the bottle headspace and the open atmosphere to reduce water evaporation (Hissler et al., 2021). Additional higher frequency precipitation samples were collected with

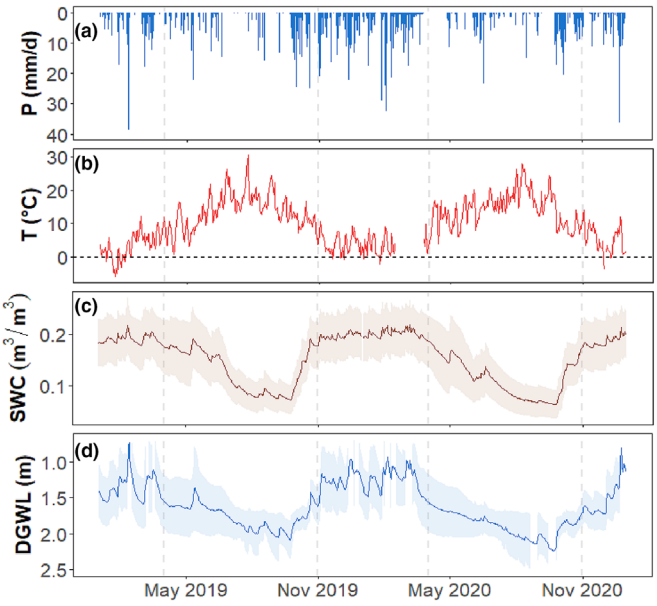

FIGURE 2 Time series of daily total precipitation amount (P) (mm/d) (a), daily average air temperature (T) (°C) (b), daily average soil water content (SWC) (m^3/m^3) (c) and daily average depth to groundwater level (DGWL) (m) (d). The shaded bands in panels c and d represent the standard deviation from the mean of all monitoring sites. The vertical dashed lines delineate the two growing seasons (1 April to 31 October).

a sequential rainfall sampler (SRS; cf. Kennedy et al., 1979) for selected periods. The SRS collected samples in approximately 2.5-mm precipitation increments, that is, a sampling interval of 23 h on average (Rodriguez & Klaus, 2019). All samples were filtered using 0.45-µm syringe filters and stored at 4°C until analysis. The $\delta^{18}O$ and $\delta^{2}H$ isotopic composition of precipitation was determined using a Los Gatos Research TIWA-45-EP. Analyses were carried out at the LIST isotopic laboratory with an analytical accuracy of 0.1‰ ($\delta^{18}O$) and 0.5‰ ($\delta^{2}H$) and a precision maintained <0.1‰ ($\delta^{18}O$) and <0.5‰ ($\delta^{2}H$) (quantified as one standard deviation of the measured samples and standards) (Hissler et al., 2021). The precipitation amount weighted SWI values were interpolated between two consecutive samples as being equal to the value of the next sample. The isotopic composition is given as the relative difference in the ratio of heavy to light isotopes of water samples (delta notation, ‰) to the Vienna Standard Mean Ocean Water (VSMOW). The local meteoric water line (LMWL; $\delta^{2}H = 7.4^{*}\delta^{18}O + 6.5$; $R^2 = 0.97$; Figure 3) was determined from the fortnightly precipitation samples taken over the period 2011–2019. This is consistent with data from the closest IAEA GNIP station in Trier (~60 km) with a LWML of $\delta^{2}H = 7.6^{*}\delta^{18}O + 3.9$ for the period 1978–2009 (Klaus et al., 2015; Stumpp et al., 2014).

2.3 | Xylem sampling

We focused our analysis on hardwood trees that dominated the catchment. We sampled sapwood xylem from beech and oak tree trunks with a Pressler corer across the catchment during the growing seasons 2019 and 2020 (Figure 1). We transferred the sapwood xylem samples into 30-mL glass vials sealed with caps and Parafilm® and kept them at −22°C until xylem water extraction.

Samples were taken during nine campaigns in 2019 (14 May, 29 May, 5 June, 26 June, 10 July, 30 August, 20 September, 2 October and 23 October) and during eight campaigns in 2020 (8 May, 25 May, 12 June, 6 July, 24 July, 11 August, 3 September and 22 September) (Table 2). For each campaign, three different zones were sampled (i.e. plateau, hillslope and riparian) in the hardwood stands (Figure 1). In each zone, we took the coordinates (*X*, *Y*) of randomly selected points. A similar number of uneven-aged beech and oak trees were then randomly selected and sampled within a 15-m radius circle around the points (*X*, *Y*). We sampled distinct trees during each campaign. For the spatial analysis, we later generated a unique partial-random set of coordinates (X_r, Y_r) for each sampled tree based on a measured angle and horizontal distance from the point (*X*, *Y*). For each campaign, we sampled on average 10 trees for each species (the number ranged between 2 and 18 individuals) (Table 2). In total, 102 and 101 samples were taken from beech and oak, respectively, in 2019, while 69 samples were taken from both tree species in 2020 (Table 2).

We measured the DBH of each tree sampled. The topographic variables at each of the sampled locations and the DBH of each of the sampled trees spanned the distributions observed in the Weierbach catchment (Table 1 and supporting information Figure S1).

2.4 | Xylem water extraction and isotopes analyses

We extracted water from xylem samples using the cryogenic vacuum distillation leak-tight line protocol (Fabiani et al., 2021; Orlowski et al., 2016). We submerged the vials containing the xylem samples in a 100°C oil bath and collected evaporated water in U-shaped tubes submerged in liquid nitrogen (−197°C) for approximately 3 h. The lines were connected to a pump that applied a vacuum to reach the suction of 0.03 hPa below which there was no water left to extract. Extraction was stopped 1 h after the suction reached the constant value of 0.03 hPa. Water was then collected using a Paster pipette, stored in 2-mL threaded vials with fixed 300-µL glass inserts and kept at 4°C before laser spectrometry analysis.

Following extraction, we measured the $\delta^{18}O$ and $\delta^{2}H$ isotopic composition of the water with a Picarro cavity ring down spectrometer (CRDS) (L2140-i, Picarro, USA) coupled with a Micro-Combustion Module TM (MCM) to remove organic compounds (ethanol, methanol and/or other biogenic volatile compounds) (Martín-Gómez et al., 2015). Each sample was analysed 10 times in a row for eradicating potential memory effect (Penna et al., 2012); an average isotope signal was determined using the last four to five measurements. Four to five standards were analysed at the start and end of each run (10 injections per standard), and five standards were analysed every ten samples (maximum of 20 injections per standard). Raw measurements of each sample were finally corrected based on linear regressions between three to four measured values of the previous and next

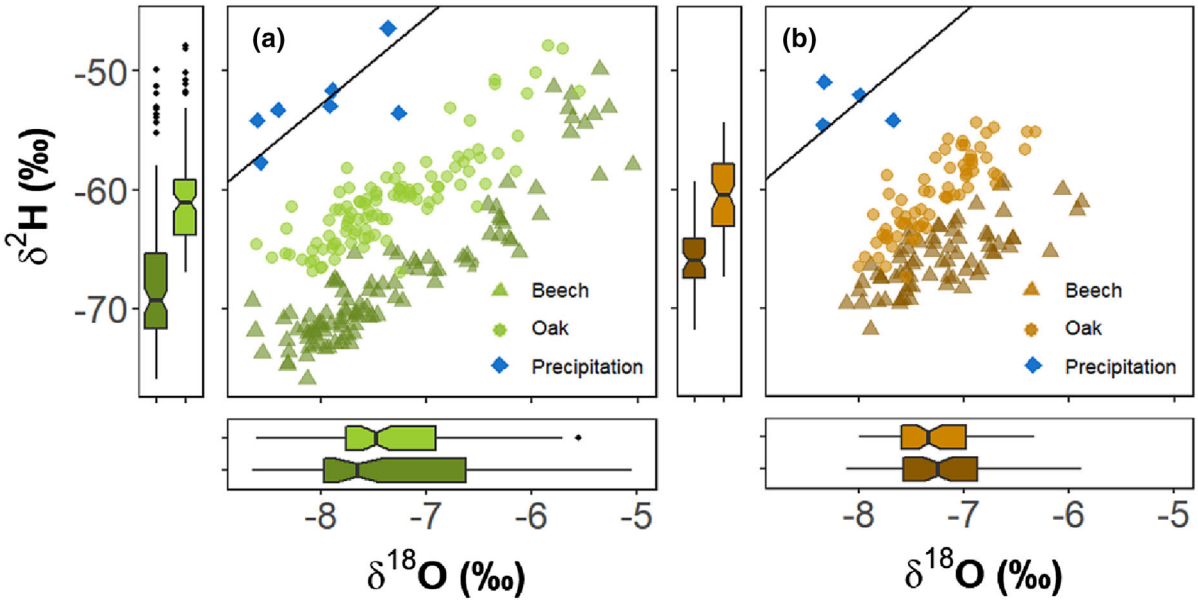

FIGURE 3 Plots showing beech and oak xylem water dual isotopes values (δ^2H and $\delta^{18}O$; ‰) for the growing seasons 2019 (a) and 2020 (b). The solid line is the local meteoric water line (LMWL) ($\delta^2H = 7.4^*\delta^{18}O + 6.5$) with the dual isotopes values of the fortnightly precipitation samples taken during each studied year. Boxplots show the median (black line in box; the notch indicate the confidence interval), the interquartile range (IQR; extent of the box), the range (lines) and the outliers (black points).

TABLE 2 Number of beech and oak sapwood xylem samples taken during each campaign for the studied years 2019 and 2020.

	2019		2020	
Campaign	**Beech**	**Oak**	**Beech**	**Oak**
1	16	15	10	10
2	18	18	10	10
3	8	8	10	10
4	12	12	8	8
5	18	18	8	8
6	10	10	7	8
7	2	3	8	8
8	7	7	8	7
9	11	11	-	-
Total	**102**	**101**	**69**	**69**

lab standards to avoid drift over the course of the analysis. The quality control lab standard water was 0.02‰ for $\delta^{18}O$ and 0.3‰ for δ^2H (Fabiani et al., 2021). The isotopic composition is given as the relative difference in the ratio of heavy to light isotopes of water samples (delta notation, ‰) to the Vienna Standard Mean Ocean Water (VSMOW).

2.5 | Data processing and statistical analyses

Data and statistical analyses were performed using R Studio Version 4.2.1 (R-Core team, 2013).

2.5.1 | Temporal variability analysis

For each species, to test if the xylem SWI data from each campaign were normally distributed, we performed the Shapiro–Wilk normality test (Shapiro & Wilk, 1965) and a graphical check. We tested the homogeneity of variance between campaigns using the Levene test homogeneity of variance (Levene, 1960) and performed a graphical check. Significance level for all tests was set at $\alpha = 0.05$. The test results generally indicated a nonnormal distribution of the xylem SWI data from each campaign and their non-homogeneous variance. We performed the nonparametric Kruskal–Wallis rank sum test (Kruskal & Wallis, 1952) to test if the xylem water isotopic composition of each species significantly varied between campaigns. We graphically evaluated the changes in median xylem SWI values between campaigns. When the Kruskal–Wallis rank sum test indicated a significant temporal change of the median SWI value, post hoc pairwise comparisons were performed using the Wilcoxon rank sum exact test (Harris & Hardin, 2013) with the Holm *p*-value adjustment method to control type I errors.

2.5.2 | Time series detrending

We combined the samples of all the campaigns to have enough samples to carry out a spatial analysis, because the 2 to 18 samples of each campaign were not sufficient for a robust spatial analysis for an individual campaign. For this, we detrended the sampling data time series using a second-order polynomial regression model using xylem SWI as a dependant variable and the sampling date as an independent

variable (supporting information Figures S2 and S3) to regroup the measured values to the same time point. The models were fitted for both monitored years individually (2019 and 2020) to account for year-specific effects in seasonality. Normality and homogeneity of variance were evaluated using the Shapiro–Wilk and Levene tests, respectively. We tested first- and second-order models and lack of fit using the *F*-test and assessed the variance explained by the models using the adjusted R^2.

2.5.3 | Spatial variability analysis

Analysis of spatial autocorrelation

We calculated the global Moran's *I* to test for the presence of spatial autocorrelation in the xylem water samples of each tree species. For this, we generated an inverse Euclidean distance matrix for each year and tree species before performing Moran's *I* test (significance level $\alpha = 0.05$) for both SWI. When this test indicated the presence of spatial autocorrelation, we constructed an empirical variogram for both SWI and species to test how the difference between samples of the same species changed as a function of the distance between them. To do so, we used 10 evenly spaced bins up to a cut-off lag distance ranging from 258 to 271 m fixed at one third of the maximum point-to-point distance (ranged from 774 to 813 m depending on the species and year) (cf. Goldsmith et al., 2018). Bin counts ranged from 41 to 324. Spherical, Exponential, Gaussian and Matérn models were fitted to the empirical variogram to identify the best models and determine the nugget, partial sill and range.

Analysis of landscape drivers

We carried out principal component regressions (PCR) (Liu et al., 2003) to reveal the landscape variables influencing xylem SWI using a combination of vegetation and topographic variables. We used species, DBH, elevation, aspect, slope, flow accumulation, curvature, TPI and TWI as independent variables (*p* predictors) and the detrended xylem SWI as dependent variable (outcome). First, we recoded the categorical variable species using dummy coding (beech: 0; oak: 1) and standardised all variables to a mean value of 0 to ensure that they all have an equal role in the principal components (PCs) generated despite differences in ranges. Then, we carried out a principal component analysis (PCA) with a 10-fold cross-validation to replace the *p* predictors by *p* PCs, each PC being a combination of the *p* predictors. We chose the *k* optimal number of PCs ($k < p$) based on which model gave the highest cumulative percentage of variance explained in the outcome, the highest correlation between the measured and the predicted values (R^2) and the smallest (root) mean square error in prediction ((R)MSEP). The selected model was fitted on a training set (70% of the original set) and tested on a test set (30% of the original set) to assess model prediction error. Using the selected model, the raw data matrix *X* with *p* predictors columns was replaced by a smaller matrix *T* with *k* PCs columns:

$$T = X * P$$

Finally, we fitted a multiple linear regression model using the non-correlated *k* PCs of *T* as predictors and the detrended xylem water isotopic composition $\hat{y}$ as the outcome.

$$\hat{y} = T * b$$

For each *k* PC, we calculated the percentage of variance in the outcome explained by each predictor as the product of the variance in the outcome explained by the PC and the loading of each predictor in the same PC. The predictors with a loading >|0.45|(Hair et al., 1998) were deemed to contribute largely to a PC. To determine the percentage of variance in the model outcome explained by each predictor, we summed the respective results of each *k* PCs of the model. We calculated the error in prediction for each sampled tree in space as the difference between the predicted and the measured value. We then tested for normally distributed errors in prediction (Shapiro & Wilk, 1965) and calculated the mean absolute error (MAE) of the model for further evaluation.

3 | RESULTS

3.1 | Precipitation and xylem SWI

Over the 2019 sampling period, precipitation median δ^2H and $\delta^{18}O$ values were −37.6‰ and −5.9‰, respectively, while median values were −32.7‰ and −4.6‰ over the 2020 sampling period (Figure 4a,b,e,f). The variability of precipitation SWI was higher over the 2019 than 2020 sampling period due to the 2019 sequential rainfall sampling that captured an isotopically depleted event in October.

Xylem water samples plotted below the LMWL determined for the study area (Figure 3). Over the 2019 sampling period, beech xylem water median δ^2H and $\delta^{18}O$ values were −69.3‰ and −7.6‰, respectively, while median values were −61.1‰ and −7.5‰ for oak xylem water (Figure 3a). Over the 2020 sampling period, beech xylem water median δ^2H and $\delta^{18}O$ values were −66.0‰ and −7.2‰, respectively, while median values were −60.5‰ and −7.3‰ for oak xylem water (Figure 3b). The variability in δ^2H and $\delta^{18}O$ of xylem water differed between tree species and years. For beech, the interquartile range (IQR) of δ^2H and $\delta^{18}O$ values was greater during 2019 (6.3‰ and 1.4‰, respectively) than 2020 (3.4‰ and 0.7‰), while the interannual variability was less pronounced for oak (IQR of 4.6‰ and 0.7‰ in 2019 for δ^2H and $\delta^{18}O$, respectively, and 5.3‰ and 0.6‰ in 2020).

3.2 | Temporal variability of xylem SWI

Between the first and last 2019 campaign, median beech xylem water $\delta^{18}O$ value changed from −7.83‰ to −5.62‰ (Figure 4c) and from −70.0‰ to −53.7‰ for δ^2H (Figure 4g). Median oak xylem water $\delta^{18}O$ value changed from −7.24‰ to −6.35‰ (Figure 4c), while δ^2H

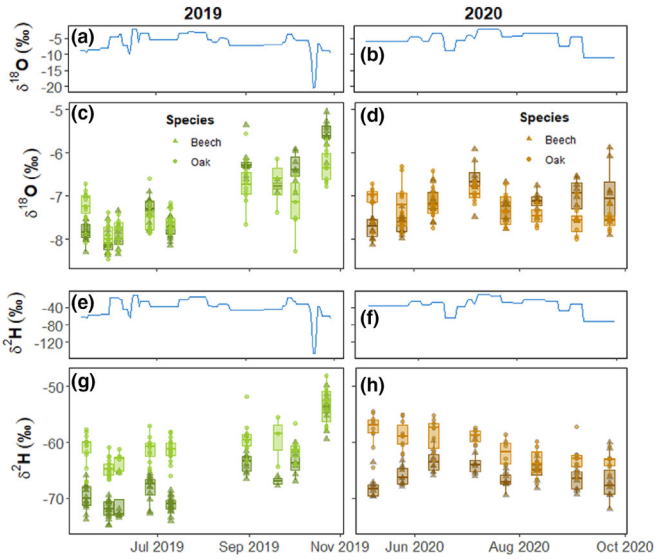

FIGURE 4 Time series of precipitation $\delta^{18}O$ (‰) (a, b), xylem water $\delta^{18}O$ (‰; boxplots, all measurements are shown with symbols) (c, d), precipitation $\delta^{2}H$ (‰) (e, f) and xylem water $\delta^{2}H$ (‰; boxplots, all measurements are shown with symbols) (g, h) over the two growing seasons 2019 and 2020. Boxplots show the median (line in box), the interquartile range (IQR; extent of the box) and the range (lines).

value changed from −60.0‰ to −51.9‰ (Figure 4g). The average change in isotope value between two campaigns was positive and higher for beech (+0.28‰ for $\delta^{18}O$, +2.04‰ for $\delta^{2}H$) than oak (+0.11‰ for $\delta^{18}O$, +1.01‰ for $\delta^{2}H$). Xylem water was significantly isotopically enriched at the end of October (ninth campaign) compared with May–July (first to fifth campaigns) for both tree species (supporting information Table S1).

Between the first and last 2020 campaign, median beech xylem water $\delta^{18}O$ value changed from −7.70‰ to −7.05‰ (Figure 4d) and from −68.4‰ to −67.6‰ for $\delta^{2}H$ (Figure 4h). Median oak xylem water $\delta^{18}O$ value changed from −6.99‰ to −7.58‰ (Figure 4d), while $\delta^{2}H$ value changed from −56.9‰ to −63.1‰ (Figure 4h). The average change in isotope value between two campaigns was positive for beech (+0.09‰ for $\delta^{18}O$, +0.11‰ for $\delta^{2}H$) and negative for oak (−0.08‰ for $\delta^{18}O$, −0.89‰ for $\delta^{2}H$). Beech xylem water was significantly isotopically enriched in June to early July (third and fourth campaigns) compared with early May (first campaign). Oak xylem water was significantly isotopically enriched in early July (fourth campaign) compared with mid-August (sixth campaign) and late September (eighth campaign) (supporting information Table S2).

3.3 | Spatial variability of xylem SWI

3.3.1 | Spatial autocorrelation

In 2019, beech and oak xylem water $\delta^{18}O$ and $\delta^{2}H$ showed significant positive spatial autocorrelation, while only $\delta^{18}O$ of beech xylem water was significantly and positively spatially autocorrelated in 2020 (Table 3). The low Moran's *I* indicated a weak spatial autocorrelation of these xylem SWI data. The empirical variograms showed a high variance in the data that was as much as the nugget size (Figure S4); this prevented the fit of any function to the variograms and the estimation of the ranges.

TABLE 3 Moran's *I* for beech and oak xylem water $\delta^{18}O$ and $\delta^{2}H$ in 2019 and 2020.

Source	$\delta^{18}O$ Moran's *I*	$\delta^{2}H$ Moran's *I*
2019		
Beech	0.15***	0.13**
Oak	0.21***	0.19***
2020		
Beech	0.13*	0.08
Oak	0.06	0.06

***$p < 0.001$, **$p < 0.01$, and *$p < 0.05$.

3.3.2 | Landscape drivers

The xylem water $\delta^{18}O$ value in 2019 was best predicted with nine PCs (MAE = 0.28, RMSEP = 0.37, MSEP = 0.14, $R^2 = 0.25$) that explained 34% of the variance in xylem water $\delta^{18}O$ across the study area. This variance was mainly explained by DBH (13.0% of the variance in xylem water $\delta^{18}O$) and to a lesser extent by TPI and flow accumulation (respectively 5.6% and 4.4% of the variance in xylem water $\delta^{18}O$) (Figure 5a). Five PCs were needed to best predict xylem water $\delta^{2}H$ value (MAE = 1.86, RMSEP = 2.50, MSEP = 6.00, $R^2 = 0.75$); they explained 76% of the variance in xylem water $\delta^{2}H$ across the study area. DBH explained a large part of the variance in xylem water $\delta^{2}H$ (46.1%), while species, slope and elevation had a lower influence (8.8%, 6.1% and 6.3% of the variance in xylem water $\delta^{2}H$, respectively) (Figure 5b). The error in prediction was randomly distributed across the study area and ranged from −0.94‰ to 0.88‰ (0–14% of error) for $\delta^{18}O$ (Figure 6a) and from −7.00‰ to 5.86‰ (0–11% of error) for $\delta^{2}H$ (Figure 6b).

The xylem water $\delta^{18}O$ value in 2020 was best predicted with five PCs (MAE = 0.28, RMSEP = 0.39, MSEP = 0.15, $R^2 = 0.39$) that explained 42% of the variance in xylem water $\delta^{18}O$ across the study area. This variance was mostly explained by DBH (24.8% of the variance in xylem water $\delta^{18}O$) and species (15.8% of the variance in xylem water $\delta^{18}O$) (Figure 5c). Five PCs were needed to best predict xylem water $\delta^{2}H$ value (MAE = 1.83, RMSEP = 2.70, MSEP = 8.00, $R^2 = 0.75$), and they explained 82% of the variance in xylem water $\delta^{2}H$ across the study area. DBH (54.6% of the variance in xylem water $\delta^{2}H$) and species (24.2% of the variance in xylem water $\delta^{2}H$) were the main variables explaining this variance (Figure 5d). The error in prediction was randomly distributed across the study area and ranged from −1.24‰ to 0.80‰ (0–19% of

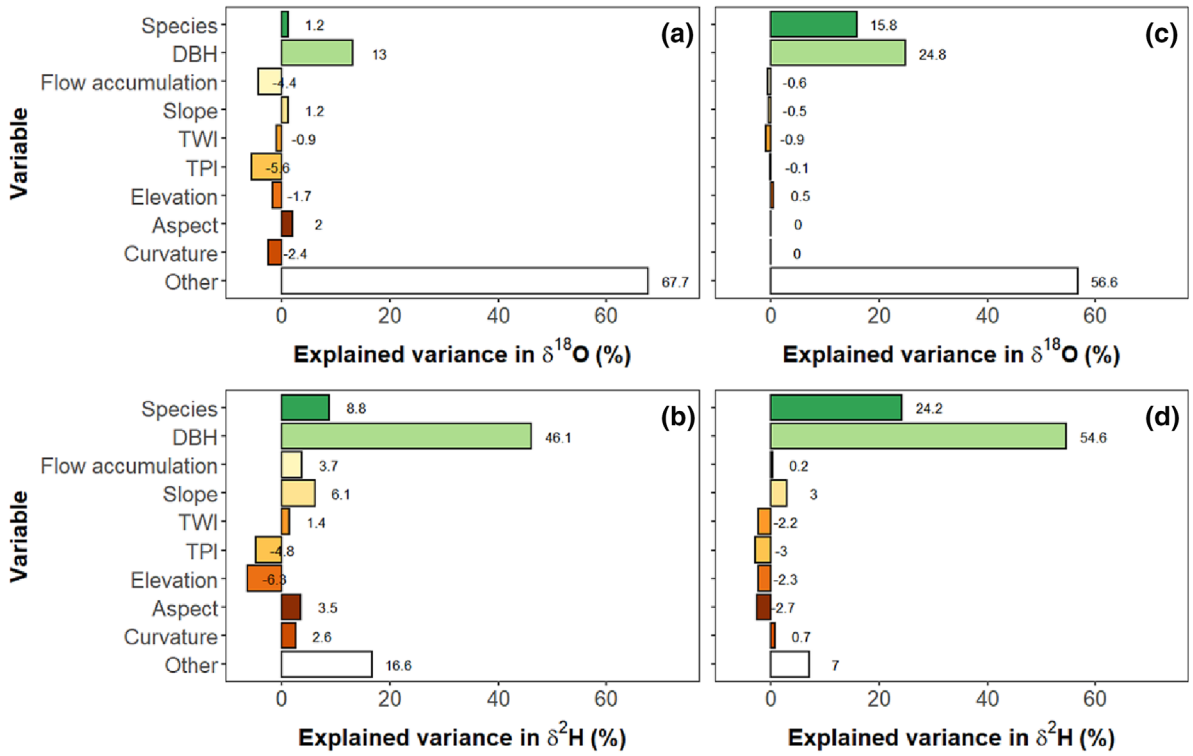

FIGURE 5 Percentage of variance (%) in xylem water $\delta^{18}O$ and $\delta^{2}H$ explained by each measured variable of the optimal model for 2019 (a, b) and 2020 (c, d) ("Other" include the nonmeasured variables). The sign of the explained variance indicates if the variable is positively or negatively correlated with the isotopic value.

error) for $\delta^{18}O$ (Figure 6c) and from −6.96‰ to 6.42‰ (0–12% of error) for $\delta^{2}H$ (Figure 6d).

4 | DISCUSSION

4.1 | Vegetation and topographic influences on the temporal and spatial variations of xylem SWI

4.1.1 | Species-specific temporal variations of xylem SWI

The different temporal variations of xylem SWI (Figure 4 and supporting information Tables S1 and S2) observed between beech and oak (both having similar DBH ranges, Table 1) during both growing seasons suggest different water use strategies. The results suggest that beech exploit shallower and seasonally less stable (due to more exposition to the evaporation-fractionation process) water sources than oak, as observed by Fabiani et al. (2021) in the study area. It is consistent with the findings of Fan et al. (2017) who reviewed tree rooting depths and showed that oak commonly has a deeper mean root system (5.23 m) than beech (0.83 m). It is also in agreement with previous studies showing that adult beech develops a rather shallow, but intensive, fine root system (Packham et al., 2012) with about two thirds of the total fine root biomass contained in the uppermost 30 cm of the soil profile in mature stands (Kirfel et al., 2019; Meier et al., 2018). In contrast, oak is considered a deep-rooted species able to access deeper subsurface water (Lanning et al., 2020), as observed by Kahmen et al. (2021) who found that oak used deeper water than beech.

The results further suggest that beech may use more various water sources than oak in response to the varying hydrometeorological conditions observed throughout the growing seasons (Figure 2). This is in line with the recent observation that beech can change its rooting patterns and water use strategy more easily than oak (Goldsmith et al., 2022). This is also consistent with the finding that beech has the same probability to use deep and shallow soil water, while oak has a higher probability to use deep than shallow soil water (Kahmen et al., 2021).

These species-specific water use strategies support the existence of different water uptake niches between the two co-occurring tree species, as recently suggested by Fabiani et al. (2021) in the study area. These water use strategies also likely demonstrate the higher niche plasticity of beech, as shown in previous research (Goldsmith et al., 2022; Kahmen et al., 2021).

4.1.2 | Dominance of DBH and species as landscape drivers of xylem SWI

The overall higher importance of DBH, and to a lower extent species, in explaining the spatial variability of xylem SWI compared with topographic variables (Figure 5) further supports that trees use a species-

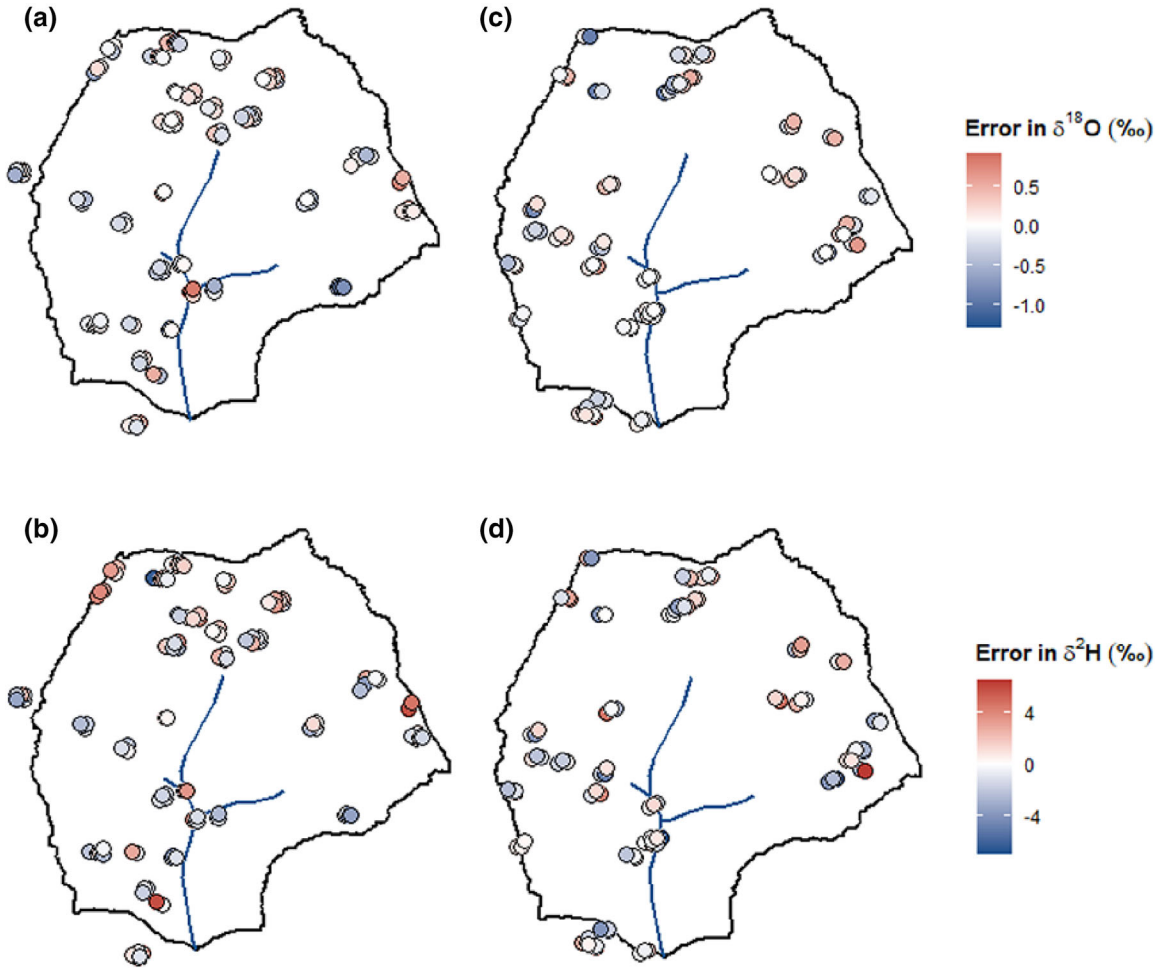

FIGURE 6 Spatial variability of the error in prediction (‰) of xylem water $\delta^{18}O$ and $\delta^{2}H$ for 2019 (a, b) and 2020 (c, d).

specific mixture of water sources from different depths. The notable influence of DBH on xylem SWI is consistent with previous studies that showed that tree diameter was associated with the depth of water uptake, with larger trees using deeper water (Dawson, 1996; Goldsmith et al., 2012; Phillips & Ehleringer, 1995). Different depths of water uptake between larger and smaller trees can lead to differences in xylem SWI values due to vertical variations in soil SWI. These variations can result from shallow soil water mixing with recent precipitation (Bertrand et al., 2014; Sprenger et al., 2018) and evaporation–fractionation of soil SWI (Bertrand et al., 2014).

The smaller influence of species in explaining the spatial variability of xylem SWI is nevertheless in line with earlier research. As discussed above, previous studies reported species-specific vertical root access (e.g. Kahmen et al., 2021) and lateral root elongation and proliferation that could lead to a greater access to soil water pools (Poot & Lambers, 2003) with depth-specific isotopic compositions (Goldsmith et al., 2012). Similar to our finding based on xylem from tree trunks, a species-specific spatial variability of xylem SWI in tree branches has previously been observed (Goldsmith et al., 2018).

The remarkable lower influence of topographic variables on xylem SWI, compared with vegetation variables, is consistent with previous findings of Gaines et al. (2016) who found a relationship between xylem SWI and tree DBH and height but no effect of the slope position on xylem SWI. Similarly, in the same study area, Fabiani et al. (2021) did not observe significant differences in xylem SWI between hillslope positions. However, these studies were carried out in areas with a small elevation range (about 50 m), and we may expect a higher contribution of topographic variables in explaining the spatial variability of xylem SWI in areas with higher topographic variations. Indeed, topography influences plant water status (Looker et al., 2018) and may, in turn, affect tree water source partitioning and associated xylem SWI in steeper areas, in addition to elevation effects of precipitation SWI.

The variance in $\delta^{2}H$ explained with the PCR models was much higher than the explained variance with models of $\delta^{18}O$ (Figure 5). The low spatial variability of xylem water $\delta^{18}O$ explained by the combination of vegetation and topographic variables used in this study demonstrates the need for further investigation. Since the data were standardised before performing the PCR, the differences in ranges between $\delta^{2}H$ and $\delta^{18}O$ (Figure 3) cannot explain these results. The findings suggest that variables other than the topographic and vegetation variables we investigated affect xylem water $\delta^{18}O$ to a higher

degree than δ^2H. The dominant influence of vegetation variables on xylem SWI indicates that vegetation processes are critical and that the differences in the variance explained by the $\delta^{18}O$ and δ^2H models may be linked to other vegetation variables (e.g. wood density, canopy density and foliage cover). Nevertheless, the random distribution of the error in prediction of both xylem water $\delta^{18}O$ and δ^2H (Figure 6) demonstrates the ability of the PCR models to reproduce the overall spatial patterns of xylem SWI across the Weierbach catchment well. Despite our sampling density that was not high enough to reveal the extent to which xylem SWI were spatially autocorrelated, the low Moran's *I* suggest that there is little spatial structuration of xylem SWI. This appears to be independent of the water availability for trees as we observed low Moran's *I* for the wetter and the drier growing seasons. Future investigations of the spatial patterns of xylem SWI should however preferably follow a spatially nested sampling design.

4.1.3 | Influence of water availability on the temporal and spatial variations of xylem SWI

The clear lower temporal variability of xylem SWI (Figure 4 and supporting information Tables S1 and S2) observed during the drier (2020) than the wetter (2019) growing season suggests that trees adapted their water uptake depths in response to drier hydrological conditions. This change is supported by the respective presence, although limited, and quasi absence of spatial autocorrelation of xylem SWI in the wetter and drier growing season(Table 3). This adaptation is also in line with the respective increase and decrease of the influence of vegetation and topographic variables on xylem SWI across space observed between the wetter and the drier growing season (Figure 5).

During the wetter growing season (2019), precipitation was approximately 100 mm higher than during the drier growing season (2020) and the water volume available for tree uptake was higher (average SWC was equal to 0.129 $m^3\ m^{-3}$ in 2019 and 0.114 $m^3\ m^{-3}$ in 2020) and more evenly distributed across the catchment. With these conditions, trees had more easily access to shallow soil water—that is seasonally more variable—(Goldsmith et al., 2012) and were less water-limited, leading to a higher temporal variability of xylem SWI compared with drier conditions. The higher use of shallow soil water by trees during wetter than drier conditions also led to a higher influence of topography on xylem SWI and to the spatial autocorrelation of these isotopes, although limited. Topographic variables such as slope influence the amount of rainwater infiltrating in soils and, in turn, soil water mixing with rainwater (Klaus et al., 2013) and in consequence soil SWI (Bertrand et al., 2014; Sprenger et al., 2018). Elevation, slope and aspect can influence air temperature and humidity that affect shallow soil SWI evaporation-fractionation (Bertrand et al., 2014). It has also been observed that the topographic index was spatially autocorrelated over a wide range of spatial extents (Cai & Wang, 2006); this may explain the spatial autocorrelation of xylem SWI observed during wetter conditions.

On the opposite, with drier conditions, trees had to adapt their water uptake strategies (e.g. depth of water uptake, related to DBH; Dawson, 1996; Goldsmith et al., 2012; Phillips & Ehleringer, 1995) and use a higher fraction of deeper and seasonally more stable water sources (Goldsmith et al., 2012). This shift in tree water source led to a lower temporal variability of xylem SWI and a higher influence of vegetation variables on xylem SWI in drier than wetter conditions. The higher use of deeper soil water by trees during the drier growing season is also in line with the quasi absence of spatial autocorrelation of xylem SWI. These observations are consistent with previous studies demonstrating that trees could shift their water sources from shallow to deep soil water (Brinkmann et al., 2019; Lanning et al., 2020) depending on the water availability to meet water requirements and regulate water status. Brinkmann et al. (2019) showed that beech was particularly able to adapt its water uptake depth depending on the SWC.

4.2 | Implications for ecohydrological and catchment studies

4.2.1 | Isotopes-based ecohydrological studies

Our results suggest that, in the Weierbach catchment, tree species and size (DBH) explained more variations in xylem SWI than the topographic variables we evaluated. Similarly, a recent study in the same area showed that species and DBH were the main drivers of the spatial variability of sap velocity (Schoppach et al., 2021).

Robust descriptions of the spatial variability in xylem SWI in ecohydrological studies are critical to provide reliable isotope-based estimates of water sources for vegetation root water uptake (Beyer & Penna, 2021). The results of our study suggest that, in the Weierbach catchment, the sampling of xylem in a set of trees with a large distribution of DBH would aid in capturing the heterogeneity of xylem SWI values across this area. Nevertheless, additional variables describing vegetation and forest structure (e.g. tree position in the canopy, crown density, leaf area index and canopy density) should be integrated to refine the understanding of vegetation influences on xylem SWI. These vegetation variables likely influence the spatial patterns of tree water uptake *via* competition between tree individuals. The role of vegetation variables in influencing xylem SWI should also be studied in a wider range of hydroclimatic and SWC conditions.

Previous analyses of the spatial patterns of xylem SWI have been carried out at the plot scale (Goldsmith et al., 2018), while other ecohydrological studies investigated the role of hillslope or topographic position (Bertrand et al., 2014; Fabiani et al., 2021; Gaines et al., 2016). These limitations may have hidden the effects of larger (for plot scale studies) or smaller scale (for hillslope scale studies) topographic heterogeneities on xylem SWI. Although topographic variables did only influence xylem SWI to a small degree in the Weierbach catchment, further examinations of the role of the position of a plant in the landscape for xylem water isotopic composition should be carried out in a wider range of landscape types (e.g. mountainous and

plateau). These investigations would improve our understanding of topographic influences on xylem SWI and our field sampling approaches.

4.2.2 | Isotopes-based catchment transit times studies

Currently, the isotopic signals of evaporation and transpiration as well as the age composition (i.e. transit time distributions) from state-of-the-art model applications (e.g. Hrachowitz et al., 2015; Rinaldo et al., 2015; Rodriguez et al., 2018, 2020; Soulsby et al., 2016; van der Velde et al., 2015; Wang et al., 2023) are more often only indirectly constrained by calibrating models to observed isotopic signals of stream flow. This implies that the relationship between the isotopic composition of the water in storage and the water that is evaporated and/or transpired from this storage remains unclear (Benettin et al., 2022). Recent development in the calibration of such models involved the use of soil and/or xylem SWI from a limited number of tree individuals, species or locations (e.g. Asadollahi et al., 2022; Knighton et al., 2019; Kuppel et al., 2018; Sprenger et al., 2022).

Our results suggest that, to better reflect the vegetation behaviour compared with these studies and to account for the importance of species in influencing xylem SWI across space, the spatially distributed xylem SWI data from our study can be used to determine species-specific isotopic signals associated with transpiration. These signals can be exploited in lumped model approaches (e.g. using a weighted mean isotopic signal of the species-specific signals) to further constrain lumped hydrological models developed for the Weierbach catchment and calibrated so far exclusively using discharge and stream SWI data (Rodriguez & Klaus, 2019). Species-specific isotopic signals associated with transpiration can also be exploited in semi-distributed models (e.g. separating beech/oak, douglas and spruce zones) (e.g. Kuppel et al., 2018).

For these purposes, a good understanding of the forest composition and structure (species, DBH) in the Weierbach catchment is required to design an optimal sampling strategy that provide a representative isotopic signature. Further work is needed in other catchments to improve the quality of the xylem SWI data used in hydrological models.

5 | CONCLUSION

In this study, the measurement of beech and oak xylem SWI during several campaigns in the Weierbach catchment revealed a higher variability over the growing season of the beech xylem water isotopic signature compared with oak. Using spatially distributed xylem SWI measurements and PCR, we identified DBH and species as the dominant variables influencing the spatial variations of xylem SWI; topographic variables had a minor role in explaining these variations. We also noted a minor presence of spatial autocorrelation between xylem samples, but our sampling density was not high enough to reveal its extent. By way of sampling xylem over two growing seasons, we observed a respective increase and decrease of the influence of vegetation and topographic variables in explaining the spatial variations of xylem SWI between the wetter and the drier seasons.

Our results suggest that, in the study area, the spatial variations of xylem SWI arise mainly from size- and species-specific as well as water availability-dependent water use strategies rather than from topographic heterogeneity. Trees can also adapt their water use strategies in response to lower water availability.

Overall, our findings highlight the importance of vegetation variables in influencing xylem SWI. We demonstrate the importance of accounting for different tree diameters and species in field sampling protocols to accurately capture the isotopic variability existing within a study area. However, there is still a need for evaluating the role of additional vegetation and forest structure variables to refine our understanding of vegetation influences on xylem SWI. This information will improve the accuracy of the lumped isotopic signal associated with transpiration used in hydrological models and will help to better predict how catchments will respond to future changes in land cover, vegetation or stand properties associated with global change.

AUTHOR CONTRIBUTIONS

Maëlle Fresne: investigation, formal analysis, visualisation and writing—original draft. **Kwok P. Chun:** conceptualisation, investigation, validation, writing—review and editing. **Markus Hrachowitz:** writing—review and editing. **Kevin J. McGuire:** writing—review and editing. **Remy Schoppach:** conceptualisation, xylem water extraction and isotopes analyses, investigation and writing—review and editing. **Julian Klaus:** conceptualisation, funding acquisition, validation, writing—review and editing and project administration.

ACKNOWLEDGEMENTS

This work was supported by the Luxembourg National Research Fund (FNR/CORE/C17/SR/11702136/EFFECT). The second author is supported by the Accelerator Programme (AP) 2022-24 and the Starter Scheme by the University of the West of England, Bristol. We thank Ginevra Fabiani, Adnan Moussa, François Barnich and Laurent Pfister for their input that helped to improve this work and manuscript. We thank the Editor and two anonymous reviewers for their comments that helped to improve this manuscript.

DATA AVAILABILITY STATEMENT

The data used in this study are the property of the Luxembourg Institute of Science and Technology (LIST) and can be obtained upon request to the corresponding author, after approval by LIST.

ORCID

Maëlle Fresne https://orcid.org/0000-0003-3304-1215
Kwok P. Chun https://orcid.org/0000-0001-9873-6240
Markus Hrachowitz https://orcid.org/0000-0003-0508-1017
Kevin J. McGuire https://orcid.org/0000-0001-5751-3956
Remy Schoppach https://orcid.org/0000-0002-9500-7007
Julian Klaus https://orcid.org/0000-0002-6301-1634

REFERENCES

Asadollahi, M., Nehemy, M. F., McDonnell, J. J., Rinaldo, A., & Benettin, P. (2022). Toward a closure of catchment mass balance: Insight on the missing link from a vegetated lysimeter. *Water Resources Research*, *58*, e2021WR030698. https://doi.org/10.1029/2021WR030698

Asano, Y., & Uchida, T. (2012). Flow path depth is the main controller of mean base flow transit times in a mountainous catchment. *Water Resources Research*, *48*, W03512. https://doi.org/10.1029/2011WR010906

Benettin, P., Rodriguez, N. B., Sprenger, M., Kim, M., Klaus, J., Harman, C. J., Van der Velde, Y., Hrachowitz, M., Botter, G., McGuire, K. J., Kirchner, J. W., Rinaldo, A., & McDonnell, J. J. (2022). Transit time estimation in catchments: Recent developments and future directions. *Water Resources Research*, *58*, e2022WR033096. https://doi.org/10.1029/2022WR033096

Bertrand, G., Masini, J., Goldscheider, N., Meeks, J., Lavastre, V., Celle-Jeanton, H., Gobat, J.-M., & Hunkeler, D. (2014). Determination of spatiotemporal variability of tree water uptake using stable isotopes ($\delta^{18}O$, $\delta^{2}H$) in an alluvial system supplied by a high-altitude watershed, Pfyn forest, Switzerland. *Ecohydrology*, *7*, 319–333. https://doi.org/10.1002/eco.1347

Beyer, M., & Penna, D. (2021). On the spatio-temporal underrepresentation of isotopic data in ecohydrological studies. *Frontiers in Water*, *3*, 16. https://doi.org/10.3389/frwa.2021.643013

Bögelein, R., Thomas, F. M., & Kahmen, A. (2017). Leaf water ^{18}O and ^{2}H enrichment along vertical canopy profiles in a broadleaved and a conifer forest tree. *Plant, Cell & Environment*, *40*, 1086–1103. https://doi.org/10.1111/pce.12895

Boisvenue, C., & Running, S. W. (2006). Impacts of climate change on natural forest productivity—Evidence since the middle of the 20th century. *Global Change Biology*, *12*, 862–882. https://doi.org/10.1111/j.1365-2486.2006.01134.x

Brinkmann, N., Eugster, W., Buchmann, N., & Kahmen, A. (2019). Species-specific differences in water uptake depth of mature temperate trees vary with water availability in the soil. *Plant Biology*, *21*, 71–81. https://doi.org/10.1111/plb.12907

Brinkmann, N., Seeger, S., Weiler, M., Buchmann, N., Eugster, W., & Kahmen, A. (2018). Employing stable isotopes to determine the residence times of soil water and the temporal origin of water taken up by *Fagus sylvatica* and *Picea abies* in a temperate forest. *The New Phytologist*, *219*, 1300–1313. https://doi.org/10.1111/nph.15255

Brutsaert, W. (1988). The parameterization of regional evaporation—Some directions and strategies. *Journal of Hydrology*, *102*(1), 409–426. https://doi.org/10.1016/0022-1694(88)90109-6

Cai, X., & Wang, D. (2006). Spatial autocorrelation of topographic index in catchments. *Journal of Hydrology*, *328*(3–4), 581–591. https://doi.org/10.1016/j.jhydrol.2006.01.009

Capell, R., Tetzlaff, D., & Soulsby, C. (2013). Will catchment characteristics moderate the projected effects of climate change on flow regimes in the Scottish highlands? *Hydrological Processes*, *27*(5), 687–699. https://doi.org/10.1002/hyp.9626

Dawson, T. E. (1996). Determining water use by trees and forests from isotopic, energy balance and transpiration analyses: The roles of tree size and hydraulic lift. *Tree Physiology*, *16*, 263–272. https://doi.org/10.1093/treephys/16.1-2.263

Fabiani, G., Schoppach, R., Penna, D., & Klaus, J. (2021). Transpiration patterns and water use strategies of beech and oak trees along a hillslope. *Ecohydrology*, *15*(2), e2382. https://doi.org/10.1002/eco.2382

Fan, Y., Miguez-Macho, G., Jobbágy, E. G., Jackson, R. B., & Otero-Casal, C. (2017). Hydrologic regulation of plant rooting depth. *Proceedings of the National Academy of Sciences*, *114*(40), 10572–10577. https://doi.org/10.1073/pnas.1712381114

Frank, D., Poulter, B., Saurer, M., et al. (2015). Water-use efficiency and transpiration across European forests during the Anthropocene. *Nature Climate Change*, *5*, 579–583. https://doi.org/10.1038/nclimate2614

Gaines, K. P., Stanley, J. W., Meinzer, F. C., & McCulloh, K. A. (2016). Reliance on shallow soil water in a mixed-hardwood forest in central Pennsylvania. *Tree Physiology*, *36*(4), 444–458. https://doi.org/10.1093/treephys/tpv113

Glaser, B., Antonelli, M., Hopp, L., & Klaus, J. (2020). Intra-catchment variability of surface saturation—Insights from physically based simulations in comparison with biweekly thermal infrared image observations. *Hydrology and Earth System Sciences*, *24*, 1393–1413. https://doi.org/10.5194/hess-24-1393-2020

Goldsmith, G. R., Allen, S. T., Braun, S., Engbersen, N., González-Quijano, C. R., Kirchner, J. W., & Siegwolf, R. T. W. (2018). Spatial variation in throughfall, soil, and plant water isotopes in a temperate forest. *Ecohydrology*, *12*(2), e2059. https://doi.org/10.1002/eco.2059

Goldsmith, G. R., Allen, S. T., Braun, S., Siegwolf, R. T. W., & Kirchner, J. W. (2022). Climatic influences on summer use of winter precipitation by trees. *Geophysical Research Letters*, *49*, e2022GL098323. https://doi.org/10.1029/2022GL098323

Goldsmith, G. R., Muñoz-Villers, L. E., Holwerda, F., McDonnell, J. J., Asbjornsen, H., & Dawson, T. E. (2012). Stable isotopes reveal linkages among ecohydrological processes in a seasonally dry tropical montane cloud forest. *Ecohydrology*, *5*(6), 779–790. https://doi.org/10.1002/eco.268

Gourdol, L., Clément, R., Juilleret, J., Pfister, L., & Hissler, C. (2021). Exploring the regolith with electrical resistivity tomography in large-scale surveys: Electrode spacing-related issues and possibility. *Hydrology and Earth System Sciences*, *25*, 1785–1812. https://doi.org/10.5194/hess-25-1785-2021

Hair, J. F., Tatham, R. L., Anderson, R. E., & Black, W. (1998). *Multivariate data analysis* (Fifth ed.). London.

Harris, T., & Hardin, J. W. (2013). Exact Wilcoxon signed-rank and Wilcoxon Mann–Whitney ranksum tests. *The Stata Journal*, *3*(2), 337–3430. https://doi.org/10.1177/1536867X1301300208

Hissler, C., Martínez-Carreras, N., Barnich, F., Gourdol, L., Iffly, J. F., Juilleret, J., Klaus, J., & Pfister, L. (2021). The Weierbach experimental catchment in Luxembourg: A decade of critical zone monitoring in a temperate forest—From hydrological investigations to ecohydrological perspectives. *Hydrological Processes*, *35*, e14140. https://doi.org/10.1002/hyp.14140

Hrachowitz, M., Fovet, O., Ruiz, L., & Savenije, H. H. G. (2015). Transit time distributions, legacy contamination, and variability in biogeochemical $1/f^{\alpha}$ scaling: How are hydrological response dynamics linked to water quality at the catchment scale? *Hydrological Processes*, *29*, 5241–5256. https://doi.org/10.1002/hyp.10546

Juilleret, J., Iffly, J. F., Pfister, L., & Hissler, C. (2011). Remarkable Pleistocene periglacial slope deposits in Luxembourg (Oesling): Pedological implication and geosite potential. *Bulletin de la Société Des Naturalistes Luxembourgeois*, *112*, 125–130.

Kahmen, A., Buser, T., Hoch, G., Grun, G., & Dietrich, L. (2021). Dynamic ^{2}H irrigation pulse labelling reveals rapid infiltration and mixing of precipitation in the soil and species-specific water uptake depths of trees in a temperate forest. *Ecohydrology*, *14*(6), e2322. https://doi.org/10.1002/eco.2322

Kendall, C., & McDonnell, J. J. (1998). *Isotopes tracers in catchment hydrology*. Elsevier Science.

Kennedy, V. C., Zellweger, G. W., & Avanzino, R. J. (1979). Variation of rain chemistry during storms at two sites in northern California. *Water Resources Research*, *15*(3), 687–702. https://doi.org/10.1029/WR015i003p00687

Kirfel, K., Hertel, D., Heinze, S., & Leuschner, C. (2019). Effects of bedrock type and soil chemistry on the fine roots of European beech—A study on the belowground plasticity of trees. *Forest Ecology and Management*, *444*, 256–268. https://doi.org/10.1016/j.foreco.2019.04.022

Klaus, J., Chun, K. P., & Stumpp, C. (2015). Temporal trends in $\delta^{18}O$ composition of precipitation in Germany: Insights from time series modelling and trend analysis. *Hydrological Processes*, *29*, 2668–2680. https://doi.org/10.1002/hyp.10395

Klaus, J., & McDonnell, J. J. (2013). Hydrograph separation using stable isotopes: Review and evaluation. *Journal of Hydrology*, *505*, 47–64. https://doi.org/10.1016/j.jhydrol.2013.09.006

Klaus, J., Zehe, E., Elsner, M., Külls, C., & McDonnell, J. J. (2013). Macropore flow of old water revisited: Experimental insights from a tile-drained hillslope. *Hydrology and Earth System Sciences*, *17*, 103–118. https://doi.org/10.5194/hess-17-103-2013

Knighton, J., Souter-Kline, V., Volkmann, T., Troch, P. A., Kim, M., Harman, C. J., Morris, C., Buchanan, B., & Walter, M. T. (2019). Seasonal and topographic variations in ecohydrological separation within a small, temperate, snow-influenced catchment. *Water Resources Research*, *55*, 6417–6435. https://doi.org/10.1029/2019WR025174

Kruskal, W. H., & Wallis, W. A. (1952). Use of ranks in one-criterion variance analysis. *Journal of the American Statistical Association*, *47*, 583–621. and errata, ibid. *48*, 907–911.

Kuppel, S., Tetzlaff, D., Maneta, M. P., & Soulsby, C. (2018). EcH2O-iso 1.0: Water isotopes and age tracking in a process-based, distributed ecohydrological model. *Geoscientific Model Development*, *11*, 3045–3069. https://doi.org/10.5194/gmd-11-3045-2018

Lanning, M., Wang, L., Benson, M., Zhang, Q., & Novick, K. A. (2020). Canopy isotopic investigation reveals different water uptake dynamics of maples and oaks. *Phytochemistry*, *175*, 112389. https://doi.org/10.1016/j.phytochem.2020.112389

Levene, H. (1960). In I. Olkin, et al. (Eds.), *Contributions to probability and statistics: Essays in honor of Harold Hotelling* (pp. 278–292). Stanford University Press.

Liu, R. X., Kuang, J., Gong, Q., & Lou, X. L. (2003). Principal component regression analysis with spss. *Computer Methods and Programs in Biomedicine*, *71*(2), 141–147. https://doi.org/10.1016/S0169-2607(02)00058-5

Looker, N., Martin, J., Hoylman, Z., Jencso, K., & Hu, J. (2018). Diurnal and seasonal coupling of conifer sap flow and vapour pressure deficit across topoclimatic gradients in a subalpine catchment. *Ecohydrology*, *11*, e1994. https://doi.org/10.1002/eco.1994

Martínez-Carreras, N., Hissler, C., Gourdol, L., Klaus, J., Juilleret, J., Iffly, J. F., & Pfister, L. (2016). Storage controls on the generation of double peak hydrographs in a forested headwater catchment. *Journal of Hydrology*, *543*, 255–269. https://doi.org/10.1016/j.jhydrol.2016.10.004

Martín-Gómez, P., Barbeta, A., Voltas, J., Peñuelas, J., Dennis, K., Palacio, S., Dawson, T. E., & Ferrio, J. P. (2015). Isotope-ratio infrared spectroscopy: A reliable tool for the investigation of plant-water sources? *The New Phytologist*, *207*, 914–927. https://doi.org/10.1111/nph.13376

Meier, I. C., Knutzen, F., Eder, L. M., Müller-Haubold, H., Goebel, M.-O., Bachmann, J., Hertel, D., & Leuschner, C. (2018). The deep root system of Fagus sylvatica on sandy soil: Structure and variation across a precipitation gradient. *Ecosystems*, *21*, 280–296. https://doi.org/10.1007/s10021-017-0148-6

Moore, G. W., & Heilman, J. L. (2011). Proposed principles governing how vegetation changes affect transpiration. *Ecohydrology*, *4*(3), 351–358. https://doi.org/10.1002/eco.232

Orlowski, N., Breuer, L., & McDonnell, J. J. (2016). Critical issues with cryogenic extraction of soil water for stable isotope analysis. *Ecohydrology*, *9*, 3–10. https://doi.org/10.1002/eco.1722

Packham, J. R., Thomas, P. A., Atkinson, M. D., & Degen, T. (2012). Biological flora of the British Isles: Fagus sylvatica. *Journal of Ecology*, *100*, 1557–1608. https://doi.org/10.1111/j.1365-2745.2012.02017.x

Penna, D., Hopp, L., Scandellari, F., Allen, S. T., Benettin, P., Beyer, M., Geris, J., Klaus, J., Marshall, J. D., Schwendenmann, L., Volkmann, T. H. M., Von Freyberg, J., Amin, A., Ceperley, N., Engel, M., Frentress, J., Giambastiani, Y., McDonnell, J. J., Zuecco, G., … Kirchner, J. W. (2018). Ideas and perspectives: Tracing terrestrial ecosystem water fluxes using hydrogen and oxygen stable isotopes–challenges and opportunities from an interdisciplinary perspective. *Biogeosciences*, *15*(21), 6399–6415. https://doi.org/10.5194/bg-15-6399-2018

Penna, D., Stenni, B., Sanda, M., Wrede, S., Bogaard, T. A., Michelini, M., Fischer, B. M. C., Gobbi, A., Mantese, N., Zuecco, G., Borga, M., Bonazza, M., Sobotková, M., Čejková, B., & Wassenaar, L. I. (2012). Technical note: Evaluation of between-sample memory effects in the analysis of $\delta^{2}H$ and $\delta^{18}O$ of water samples measured by laser spectroscopes. *Hydrology and Earth System Sciences*, *16*, 3925–3933. https://doi.org/10.5194/hess-16-3925-2012

Pfister, L., Martínez-Carreras, N., Hissler, C., Klaus, J., Carrer, G. E., Stewart, M. K., & McDonnell, J. J. (2017). Bedrock geology controls on catchment storage, mixing, and release: A comparative analysis of 16 nested catchments. *Hydrological Processes*, *31*(10), 1828–1845. https://doi.org/10.1002/hyp.11134

Phillips, S. L., & Ehleringer, J. R. (1995). Limited uptake of summer precipitation by bigtooth maple (Acer grandidentatum Nutt) and Gambel's oak (Quereus gambelii Nutt). *Trees*, *9*, 214–219. https://doi.org/10.1007/BF00195275

Poot, P., & Lambers, H. (2003). Are trade-offs in allocation pattern and root morphology related to species abundance? A congeneric comparison between rare and common species in the south-western Australian flora. *Journal of Ecology*, *91*, 58–67. https://doi.org/10.1046/j.1365-2745.2003.00738.x

R-Core Team. (2013). *R: A language and environment for statistical computing*. R Foundation for Statistical Computing. http://www.R-project.org/

Rinaldo, A., Benettin, P., Harman, C. J., Hrachowitz, M., McGuire, K. J., Van Der Velde, Y., Bertuzzo, E., & Botter, G. (2015). Storage selection functions: A coherent framework for quantifying how catchments store and release water and solutes. *Water Resources Research*, *51*(6), 4840–4847. https://doi.org/10.1002/2015WR017273

Rodriguez, N. B., Benettin, P., & Klaus, J. (2020). Multimodal water age distributions and the challenge of complex hydrological landscapes. *Hydrological Processes*, *34*, 2707–2724. https://doi.org/10.1002/hyp.13770

Rodriguez, N. B., & Klaus, J. (2019). Catchment travel times from composite StorAge selection functions representing the superposition of streamflow generation processes. *Water Resources Research*, *55*(11), 9292–9314. https://doi.org/10.1029/2019WR024973

Rodriguez, N. B., McGuire, K. J., & Klaus, J. (2018). Time-varying storage–water age relationships in a catchment with a Mediterranean climate. *Water Resources Research*, *54*, 3988–4008. https://doi.org/10.1029/2017WR021964

Rodriguez-Iturbe, I. (2000). Ecohydrology: A hydrologic perspective of climate-soil-vegetation dynamies. *Water Resources Research*, *36*(1), 3–9. https://doi.org/10.1029/1999WR900210

Schoppach, R., Chun, K. P., He, Q., Fabiani, G., & Klaus, J. (2021). Species-specific control of DBH and landscape characteristics on tree-to-tree variability of sap velocity. *Agricultural and Forest Meteorology*, *307*, 108533. https://doi.org/10.1016/j.agrformet.2021.108533

Sevruk, B., Ondras, M., & Chvíla, B. (2009). The WMO precipitation measurement intercomparisons. *Atmospheric Research*, *92*(3), 376–380. https://doi.org/10.1016/j.atmosres.2009.01.016

Shapiro, S. S., & Wilk, M. B. (1965). An analysis of variance test for normality (complete samples). *Biometrika*, *52*, 591–611. https://doi.org/10.1093/biomet/52.3-4.591

Snelgrove, J. R., Buttle, J. M., Kohn, M. J., & Tetzlaff, D. (2021). Co-evolution of xylem water and soil water stable isotopic composition in a northern mixed forest biome. *Hydrology and Earth System Sciences*, *25*, 2169–2186. https://doi.org/10.5194/hess-25-2169-2021

Soulsby, C., Birkel, C., & Tetzlaff, D. (2016). Characterizing the age distribution of catchment evaporative losses. *Hydrological Processes*, *30*(8), 1308–1312. https://doi.org/10.1002/hyp.10751

Sprenger, M., Leistert, H., Gimbel, K., & Weiler, M. (2016). Illuminating hydrological processes at the soil-vegetation-atmosphere interface with water stable isotopes. *Reviews of Geophysics*, *54*, 674–704. https://doi.org/10.1002/2015RG000515

Sprenger, M., Llorens, P., Gallart, F., Benettin, P., Allen, S. T., & Latron, J. (2022). Precipitation fate and transport in a Mediterranean catchment through models calibrated on plant and stream water isotope data. *Hydrology and Earth System Sciences*, *26*, 4093–4107. https://doi.org/10.5194/hess-26-4093-2022

Sprenger, M., Tetzlaff, D., Buttle, J., Carey, S. K., McNamara, J. P., Laudon, H., Shatilla, N. J., & Soulsby, C. (2018). Storage, mixing, and fluxes of water in the critical zone across northern environments inferred by stable isotopes of soil water. *Hydrological Processes*, *32*(12), 1720–1737. https://doi.org/10.1002/hyp.13135

Stumpp, C., Klaus, J., & Stichler, W. (2014). Analysis of long-term stable isotopic composition in German precipitation. *Journal of Hydrology*, *517*, 351–361. https://doi.org/10.1016/j.jhydrol.2014.05.034

Tetzlaff, D., Buttle, J., Carey, S. K., Kohn, M. J., Laudon, H., McNamara, J. P., Smith, A., Sprenger, M., & Soulsby, C. (2020). Stable isotopes of water reveal differences in plant–soil water relationships across northern environments. *Hydrological Processes*, *35*(1), e14023. https://doi.org/10.1002/hyp.14023

Tetzlaff, D., Soulsby, C., Buttle, J., Capell, R., Carey, S. K., Laudon, H., McDonnell, J. J., McGuire, K. J., Seibert, J., & Shanley, J. (2013). Catchments on the cusp? Structural and functional change in northern ecohydrology. *Hydrological Processes*, *27*, 766–774. https://doi.org/10.1002/hyp.9700

Van Der Velde, Y., Heidbüchel, I., Lyon, S. W., Nyberg, L., Rodhe, A., Bishop, K., & Troch, P. A. (2015). Consequences of mixing assumptions for time-variable travel time distributions. *Hydrological Processes*, *29*(16), 3460–3474. https://doi.org/10.1002/hyp.10372

Wang, S., Hrachowitz, M., Schoups, G., & Stumpp, C. (2023). Stable water isotopes and tritium tracers tell the same tale: No evidence for underestimation of catchment transit times inferred by stable isotopes in SAS function models. *Hydrology and Earth System Sciences Discussions* [preprint], in review, 1–44. https://doi.org/10.5194/hess-2022-400

Wilson, J. P., & Gallant, J. C. (2000). *Terrain analysis: Principles and applications*. John Wiley & Sons.

SUPPORTING INFORMATION

Additional supporting information can be found online in the Supporting Information section at the end of this article.

How to cite this article: Fresne, M., Chun, K. P., Hrachowitz, M., McGuire, K. J., Schoppach, R., & Klaus, J. (2023). Importance of tree diameter and species for explaining the temporal and spatial variations of xylem water $\delta^{18}O$ and $\delta^{2}H$ in a multi-species forest. *Ecohydrology*, e2545. https://doi.org/10.1002/eco.2545